Nov 6th, 12:00 AM - 12:00 AM

Bond-Slip Characteristics between Cold-Formed Metal and Concrete

Yazdan Majdi

Cheng-Tzu Thomas Hsu

Sun Punurai

Twenty-Second International Specialty Conference on Cold-Formed Steel Structures
St. Louis, Missouri, USA, November 5 & 6, 2014

Bond-Slip Characteristics between Cold-Formed Metal and Concrete

Yazdan Majdi[1], Cheng-Tzu Thomas Hsu[2], and Sun Punurai[3]

Abstract

Composite action in systems consisting of steel and concrete depends on an effective shear-transfer mechanism between the two materials. Such mechanism for smooth steel surfaces inside concrete will be limited to the bond-slip behavior at the steel/concrete interfaces. This research investigates the bond-slip behavior of galvanized cold-formed (light gauge) steel profiles embedded in concrete. A new innovative pull-out test is presented and global bond-slip curves for different values of concrete strength are obtained from such tests. Next, through an innovative procedure, mathematical equations and a few points from the experimental global bond-slip curves are used to develop a bi-linear local bond-slip model which represents the local bond-slip behavior. Then by curve fitting, empirical equations are proposed to determine the suggested model's parameters based on concrete compressive strength. Finally, validity of the proposed model is explored by two methods: 1) by comparing its resulting global bond-slip graphs from analytical equations with test results. 2) by comparing its resulting global bond-slip graphs from finite element modeling with test results.

[1] PhD, PE, Structural Engineer, Arup, New York, NY, USA
[2] PhD, PEng, Professor and Director of High Performance Concrete Structures Laboratory, Department of Civil and Environmental Engineering, New Jersey Institute of Technology, Newark, NJ, USA
[3] PhD, Chief of Transport System - Research and Development Section, Expressway Authority of Thailand, Bangkok, Thailand

Introduction

While there can be found ample scientific documents in the literature regarding the bond-slip behavior between ribbed (deformed) rebars or fiber reinforced polymer (FRP) sheets and concrete, very few focus on bond-slip of plain surface steel plates. With the recent growth of light gauge steel use in composite constructions; (Hsu, et al, 2012), a necessity for studying the behavior of light gauge steel profiles embedded in concrete has become significant.

The aim of this research is to develop and verify a local bond-slip model which can represent the behavior of cold-formed (light gauge) galvanized profiles and plates embedded in normal weight normal strength concrete. The paper begins with setting up and solving the bond-slip governing differential equation based on a bi-linear behavior and specific boundary conditions to obtain the necessary mathematical equations, then a new and unique test set-up is introduced for the experimental studies and the results are presented. Afterwards, a new innovative procedure is described and followed to calibrate the mathematical equations based on pieces of information from the test data and from there; a local bond-slip model is developed. Finally, the suggested model is verified using two methods.

Bond-slip Tests

Experimental studies on bond-slip behavior are often conducted through the pull-out test. Generally in this test, a steel member is partially embedded into a concrete block. While the concrete block is kept fixed in place, the steel member is pulled out by a gradually increasing force. In a push/pull-out test, the concrete block is fixed at the plate embedment side such that the tension increase on steel plate causes compressive stress in concrete. In a pull/pull-out test, however, the concrete block is fixed on the opposite side of plate embedment and is consequently subjected to tensile stresses. Results from the pull-out test with an easy set-up will be a load-displacement curve in which the load represents total bond force and the displacement represents slip of the plate at the beginning of embedment in concrete. This load-displacement curve can be referred to as "global bond-slip behavior" and can be used to predict the local bond-slip behavior through an analytical procedure.

Bond-slip Governing Differential Equation for a Pull/Pull-out Test

In a pull/pull-out test both embedded steel and concrete block are in tension. A general situation for this test is shown in Figure 1. Referring to that figure, from

the conditions of equilibrium and assuming a linear behavior for materials, bond-slip governing differential equation for a pull/pull-out test can be obtained:

$$\frac{d^2\delta}{dx^2} - \lambda_0^2.\tau = 0 \quad (1)$$

$$\lambda_0^2 = \frac{2}{t_s}\left(\frac{1}{E_s} + \frac{A_s}{E_c A_c}\right) \quad (2)$$

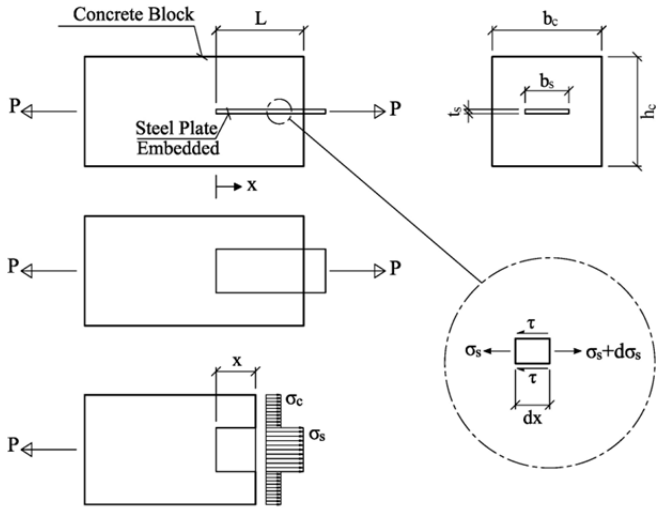

Figure 1 General condition in a pull/pull-out test.

Slip can be defined as: $\delta = u_s - u_c$ Where u_s and u_c are displacements of steel and concrete respectively. P is a pull-out force, σ_s and σ_c are normal stresses in steel and concrete respectively, τ is the bond stress, As = $b_s.t_s$, $A_c = b_c\ h_c.$, t_s is the thickness of the embedded steel sheet (or profile), b_c and h_c are the width and height of the concrete block section and b_s is the total length of the mid-line of the light gauge steel's cross section. Note bond stress and slip vary over the length of embedment. In this research, value of slip at x=L is shown with d.

Other researchers have achieved similar governing differential equations with different coefficients for push/pull-out tests (Yuan, et al, 2001).

To solve the governing differential equation, a general relationship between the bond stress (τ) and slip (δ) should be assumed. In this research the local bond-slip behavior between the cold-formed steel and concrete is assumed to have a

bi-linear shape as shown in Figure 2.

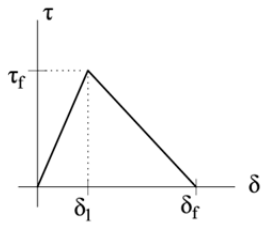

Figure 2 Assumed local bond-slip relationship

In a pull-out test, depending on the value of slip, the following cases will be observed:

Case 1: initially for small values of δ, all bond elements over the embedded surface are in the ascending zone.

Case 2: for large values of δ, slip in all bond elements will be more than δ_1 which means all elements have entered the softening zone.

Case 3: for medium range values of δ, slip in some bond elements exceeds δ_1 while in other elements slip is still less than δ_1. This means some bond elements are in the ascending branch and some are in the softening zone.

Solution for Case 1:

$$\delta = A\cosh(\lambda_1 x) + B\sinh(\lambda_1 x) \tag{3}$$

$$\lambda_1^2 = \frac{\tau_f}{\delta_1}\,\lambda_0^2 \tag{4}$$

$$B = -\frac{P}{\lambda_1 E_c A_c} \tag{5}$$

$$A = \frac{P}{\lambda_1}\left[\frac{t_s\lambda_0^2}{2A_s\sinh(\lambda_1 L)} + \frac{\cosh(\lambda_1 L) - 1}{A_c E_c \sinh(\lambda_1 L)}\right] \tag{6}$$

Solution for Case 2:

$$\delta = C\sin(\lambda_2 x) + D\cos(\lambda_2 x) + \delta_f \tag{7}$$

$$\lambda_2^2 = \frac{\tau_f}{\delta_f - \delta_1}\,\lambda_0^2 \tag{8}$$

$$C = -\frac{P}{\lambda_2 E_c A_c} \tag{9}$$

$$D = \frac{P}{\lambda_2}\left[\frac{1-\cos(\lambda_2 L)}{A_c E_c \sin(\lambda_2 L)} - \frac{t_s \lambda_0^2}{2A_s \sin(\lambda_2 L)}\right] \tag{10}$$

Solution for Case 3:

In this case, some elements are in the ascending zone and some are in the softening zone of the bi-linear constitutive model. Defining "a" as the "softening length", the solution for this case can be obtained as:

$$\delta_I = A' \cosh(\lambda_1 x) + B' \sinh(\lambda_1 x) \quad (\text{for } 0 \le x \le L - a) \tag{11}$$

$$\delta_{II} = C' \sin[\lambda_2 (x - L + a)] + D' \cos[\lambda_2 (x - L + a)] + \delta_f \quad (\text{for } L - a \le x < L) \tag{12}$$

$$B' = -\frac{P}{\lambda_1 E_c A c} \tag{13}$$

$$A' = \frac{\delta_1}{\cosh[\lambda_1 (L-a)]} + \frac{P}{\lambda_1 E_c A_c} \tanh[\lambda_1 (L-a)] \tag{14}$$

$$D' = \delta_1 - \delta_f \tag{15}$$

$$C' = \frac{P}{\lambda_2}\left[\frac{t_s \lambda_0^2}{2A_s} - \frac{1}{A_c E_c}\right] \sec(\lambda_2 a) + (\delta_1 - \delta_f)\tan(\lambda_2 a) \tag{16}$$

Based on the obtained solution, distribution of bond stress over the embedded length is illustrated in Figure 3 for all 3 cases.

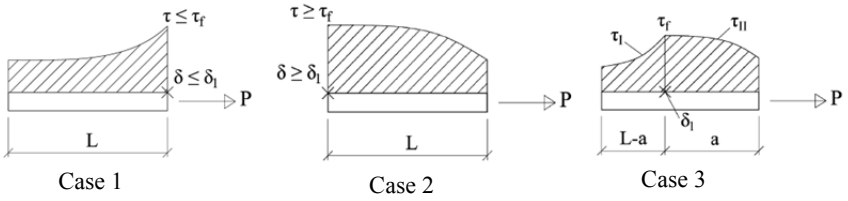

Figure 3 Distribution of bond stress in the 3 cases (one side shown only)

One should note that in Case 3, a = 0 represents the end of Case 1 where the first bonding element has just entered the softening branch whereas a = L represents the beginning of Case 2 where the last bonding element has entered softening

branch. Thus, it is reasonable to assume that the maximum transferrable load in the test, P_{max}, will be achieved in Case 3.

Referring to Figure 3, P can be obtained as a function of "a" by writing the equilibrium condition for the whole embedded plate

$$P = \frac{2b_s\left[\frac{\tau_f}{\lambda_2}\tan(\lambda_2 a) + \frac{\tau_f}{\lambda_1}\tanh[\lambda_1(L-a)]\right]}{1 - \frac{2b_s}{\lambda_0^2}\left[\Psi_2 + \Psi_1(1-\cos(\lambda_2 a))\right]} \tag{17}$$

$$\Psi_1 = \left[\frac{1}{A_c E_c} - \frac{\lambda_0^2}{2b_s}\right]\sec(\lambda_2 a) \tag{18}$$

$$\Psi_2 = \frac{1}{A_c E_c}[1 - \cosh[\lambda_1(L-a)] + \tanh[\lambda_1(L-a)]\sinh[\lambda_1(L-a)]] \tag{19}$$

In order to find P_{max}, one can apply: $\frac{dP}{da} = 0$

Experimental Program

In the experimental part of this research, an innovative set-up has been devised to perform pull/pull-out tests. The system is fully symmetrical which avoids bending moments due to unintentional eccentricities. The experimental set-up is shown in Figure 4.

Neglecting the slip of cold-formed channels on the 8 inch embedment side, global slip of channels on the 3 inch embedment side is equal to increase of distance between the two concrete blocks minus the elongation of steel channels over their free length between the blocks. For the purpose of measurement, an extensometer is attached to the concrete blocks to measure the distance variation between them and a strain gauge is placed on each furring channel to measure channels elongations over the 3" gap between the blocks.

Data from a series of four tests with the described set-up are used for processing in this research. In each test, a different value of concrete strength has been used while all other conditions are the same. Tests are designated as T1, T2, T3 and T4. The global bond-slip behavior obtained from each test is shown in Figure 5. All tests are performed in a stroke control manner with displacement rate of 0.01 in/min.

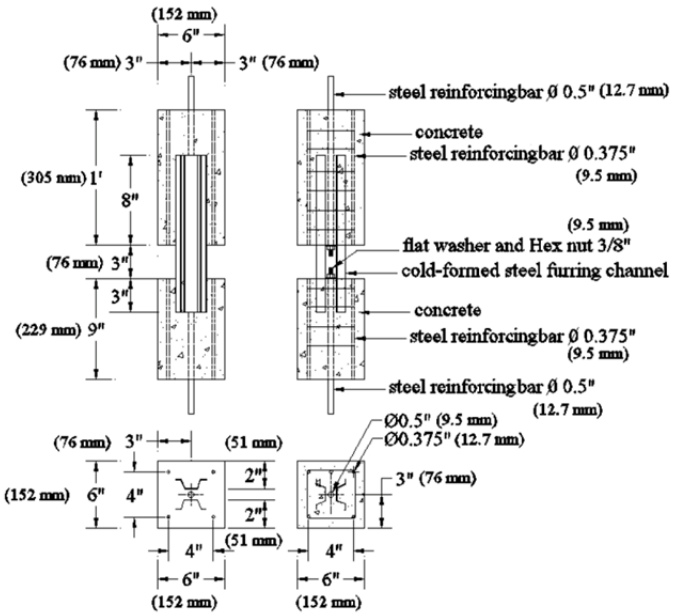

Figure 4 New innovative pull/pull-out test set-up

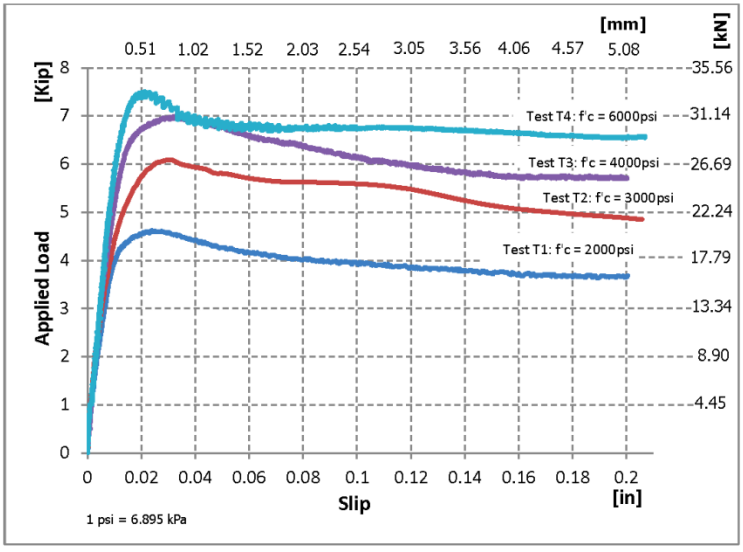

Figure 5 Results of the pull-out tests

Table 1 Geometric and Material Properties for the Pull-out Tests

Parameter	Unit	Value	Remarks
b_c	in (mm)	*6 (152.4)*	Width of concrete block section
h_c	in (mm)	*6 (152.4)*	Height of concrete block section
b_s	in (mm)	*8 (203.2)*	Twice the length of cross section's mid-line for a furring channel.
t_s	in (mm)	*0.0312 (0.7925)*	Thickness of furring channels
E_c	ksi (MPa)	$57\sqrt{f_c'}$ $(4700\sqrt{f_c'})$	Modulus of elasticity for concrete according to ACI code, f'c is in psi (MPa)
E_s	ksi (GPa)	*29000 (199.95)*	Modulus of elasticity for furring channels
L	in (mm)	*3 (76.2)*	Embedment length

Determination of the Unknown Parameters in the Model

The three unknowns of the assumed local bond-slip behavior, τ_f, δ_1 and δ_f can be obtained using some information from pull-out tests results. In this research, the following step by step procedure is proposed to determine the model's unknowns from the results of pull/pull-out test:

For each pull-out test, value of τ_f is arbitrarily chosen as the maximum average bond stress obtained from the experiment. This means that if the maximum transferable load in the global bond-slip curve is equal to P'_{max}, one has:

$$\tau_f = \frac{P'_{max}}{2b_s L} \tag{20}$$

where b_s and L are width and length of the embedded plate, respectively. Factor 2 in the denominator accounts for the fact that the bond stress is distributed over 2 surfaces of the embedded plate.

As the second step, a point from the experimental global bond-slip curve is selected. This point should be chosen from somewhere at the beginning of the global bond-slip curve for which it can be assumed all bond elements over the embedded surface are in the ascending portion. For this point, the global slip is referred to as d_1 and the applied load is referred to as P_1. Equations obtained for

Case 1 can be applied to this point.

As the final step, another point from the experimental global bond-slip curve is selected. This point should be chosen from somewhere in the descending portion of the global bond-slip curve, far enough from the point of maximum load, for which it can be assumed all bond elements over the embedded surface are in the softening portion of the local bond-slip relationship. For this point, the global slip is referred to as d_2 and the applied load is referred to as P_2. Equations for Case 2 can be applied to this point.

Table 2 Parameters of Local Bond-slip Model Determined from Pull-out Tests

Test No.	f'_c psi (MPa)	P'_{max} kip (kN)	d_1 in (mm)	P_1 kip (kN)	d_2 in (mm)	P_2 kip (kN)	τ_f psi (MPa)	δ_1 in (mm)	δ_f in (mm)
1	2000 (13.789)	4.608 (20.497)	0.0099 (0.2515)	3.951 (17.574)	0.168 (4.2672)	3.699 (16.454)	96 (0.662)	0.0109 (0.2769)	0.8046 (20.437)
2	3000 (20.684)	6.096 (27.116)	0.0068 (0.1727)	3.502 (15.577)	0.1546 (3.9268)	5.1 (22.686)	127 (0.876)	0.011 (0.2794)	0.8855 (22.492)
3	4000 (27.579)	6.912 (30.746)	0.0071 (0.1803)	4.043 (17.984)	0.1714 (4.3536)	5.725 (25.466)	144 (0.993)	0.0112 (0.2845)	0.9395 (23.863)
4	6000 (41.368)	7.488 (33.308)	0.0081 (0.2057)	4.995 (22.218)	0.1097 (2.7864)	6.754 (30.043)	156 (1.076)	0.0111 (0.2819)	1.0072 (25.583)

Table 3 Maximum Transferrable Load from Analytical Model (P_{max}) and Experiment (P'_{max})

Test No.	f'_c psi (MPa)	P'_{max} kip (kN)	P_{max} kip (kN)	a_m in (mm)
1	2000 (13.789)	4.608 (20.497)	4.607 (20.493)	2.78 (70.612)
2	3000 (20.684)	6.096 (27.116)	6.093 (27.103)	2.818 (71.577)
3	4000 (27.579)	6.912 (30.746)	6.909 (30.733)	2.84 (72.136)
4	6000 (41.368)	7.488 (33.308)	7.484 (33.290)	2.868 (72.847)

Proposed Local Bond-Slip Relationship

The procedure described in the previous section is employed in the following to determine the unknowns of the local bond-slip behavior for the pull-out tests 1 through 4. Values used in the calculations for geometric and material properties are in accordance with the performed pull-out tests and are listed in Table 1. By using the procedure proposed in the previous section, unknown parameters of the local bond-slip relationship can be determined for each pull-out test. They are presented in Table 2. From that table, one can observe that δ_1 is almost the same for all pull-out tests. Thus, a constant value of $\delta_1 = 0.011$ inch (0.279 mm) is proposed for concrete strength in the range 2000 to 6000 psi (13.789 to 41.368 MPa). Furthermore, by plotting the values of τ_f and δ_f versus $\sqrt{f'_c}$, one obtains the following equations to determine τ_f and δ_f for different values of f'c in range of 2000 to 6000 psi (13.789 to 41.3685 MPa):

$$\tau_f = -0.054\, f'_c + 8.433\sqrt{f'_c} - 173 \tag{21}$$

$$\delta_f = 0.369\, \ln\left(\sqrt{f'_c}\right) - 0.595 \tag{22}$$

where f'c and τ_f are in psi and δ_f is in inch. In SI units, the above equations will take the form:

$$\tau_f = -0.054\, f'_c + 0.7\sqrt{f'_c} - 1.193$$

$$\delta_f = 9.373\, \ln\left(\sqrt{f'_c}\right) + 8.213$$

where f'c and τ_f are in MPa and δ_f is in mm.

Verification by Analytical Equations

In order to conduct analytical verification, for each pull-out test, by having τ_f, δ_1 and δ_f, the values of P (applied load) can be plotted versus d in the solutions obtained from the bond-slip differential equation. The resulting graph will be the global bond-slip graph based on analytical (mathematical) equations which can be compared with the experimental graph. Since the solution to the differential equation has three parts, the analytical P-d curve will have 3 portions:

$$P = \frac{\lambda_1 d}{\left[\frac{t_s \lambda_0^2}{2A_s \sinh(\lambda_1 L)} + \frac{\cosh(\lambda_1 L) - 1}{A_c E_c \sinh(\lambda_1 L)}\right]\cosh(\lambda_1 L) - \frac{\sinh(\lambda_1 L)}{E_c A_c}} \qquad \{d \le \delta 1\} \tag{23}$$

$$P = \frac{\delta_f - (\delta_1 - \delta_f)\tan(\lambda_2 a)\sin(\lambda_2 a) - (\delta_1 - \delta_f)\cos(\lambda_2 a) + d}{\frac{1}{\lambda_2}\left(\frac{t_s\lambda_0^2}{2A_s} - \frac{1}{A_c E_c}\right)\tan(\lambda_2 a)} \quad \{\delta_1 \leq d \leq \delta_f \,\&\, 0 \leq a \leq L\} \tag{24}$$

$$P = \frac{\lambda_2\,(\delta_f - d)}{\frac{\sin(\lambda_2 L)}{E_c A_c} - \left[\frac{1-\cos(\lambda_2 L)}{A_c E_c \sin(\lambda_2 L)} - \frac{t_s\lambda_0^2}{2A_s \sin(\lambda_2 L)}\right]\cos(\lambda_2 L)} \quad \{\delta_1 \leq d \leq \delta_f \,\&\, \delta_1 \leq \delta(0)\} \tag{25}$$

Further, Equation (17) can be used to determine the maximum analytical transferrable load. In Table 3, analytical values of the maximum transferable load are compared with experimental ones.

Verification by Finite Element Modeling

The objective of finite element modeling here is to simulate the pull-out tests and obtain their global bond-slip behavior by using the proposed local bond-slip relationship. The obtained global bond-slip graph can then be compared with the experimental graph. ANSYS software package is used for the present finite element modeling and analysis. ANSYS Contact Technology is specifically used for the purpose of modeling the bond-slip behavior with CONTA173/TARGE170 elements (Ansys Inc., 2009a).

Each pull-out test, from T1 to T4 is simulated in a three dimensional ANSYS model. For the concrete blocks, 8 node brick elements (SOLID65) are used. The furring channel has been modeled using 4 node shell elements (SHELL181). (Ansys Inc., 2009b).

Finite element configuration of the pull-out tests is depicted in Figure 6. Finite element simulation is performed for all 4 pull-out tests. Models are analyzed by gradually pulling out the furring channels in a displacement controlled loading. At each stage of loading, the global displacement and the total load applied to the system are recorded to obtain a global bond-slip behavior. Note that through finite element modeling, an actual stress and slip distribution can also be obtained. Figure 7 illustrate the distribution of bond stress over the embedded length for test T3 at P = 4 kips.

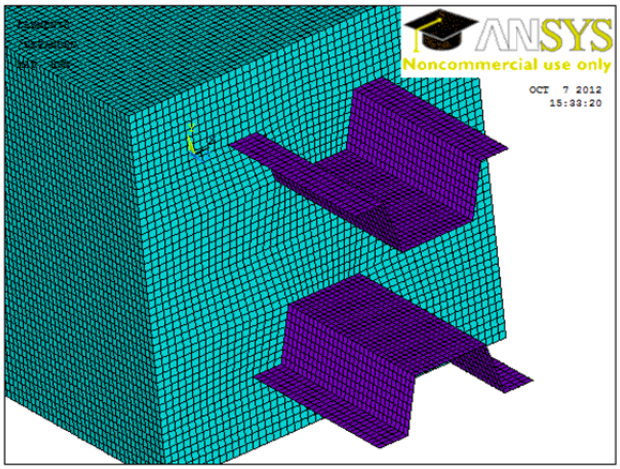

Figure 6 Finite element simulation of the pull-out test

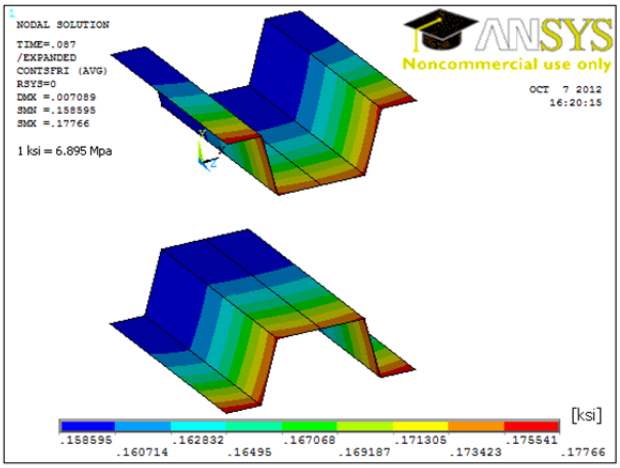

Figure 7 Distribution of bond stress over the embedded length

Results of Verifications

Global bond-slip behaviors obtained from analytical equations and finite element modeling are compared with the experimental graphs from tests in Figures 8. As observed, both verification methods have achieved excellent agreements with the test results.

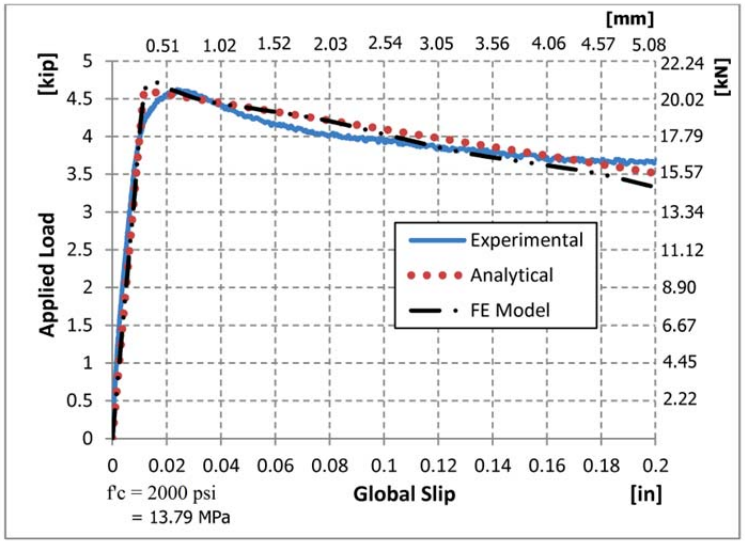

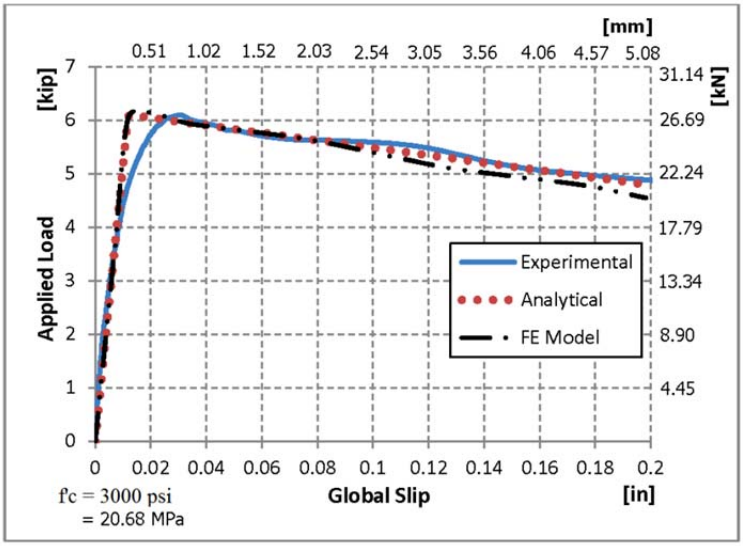

Figure 8a Results of verification

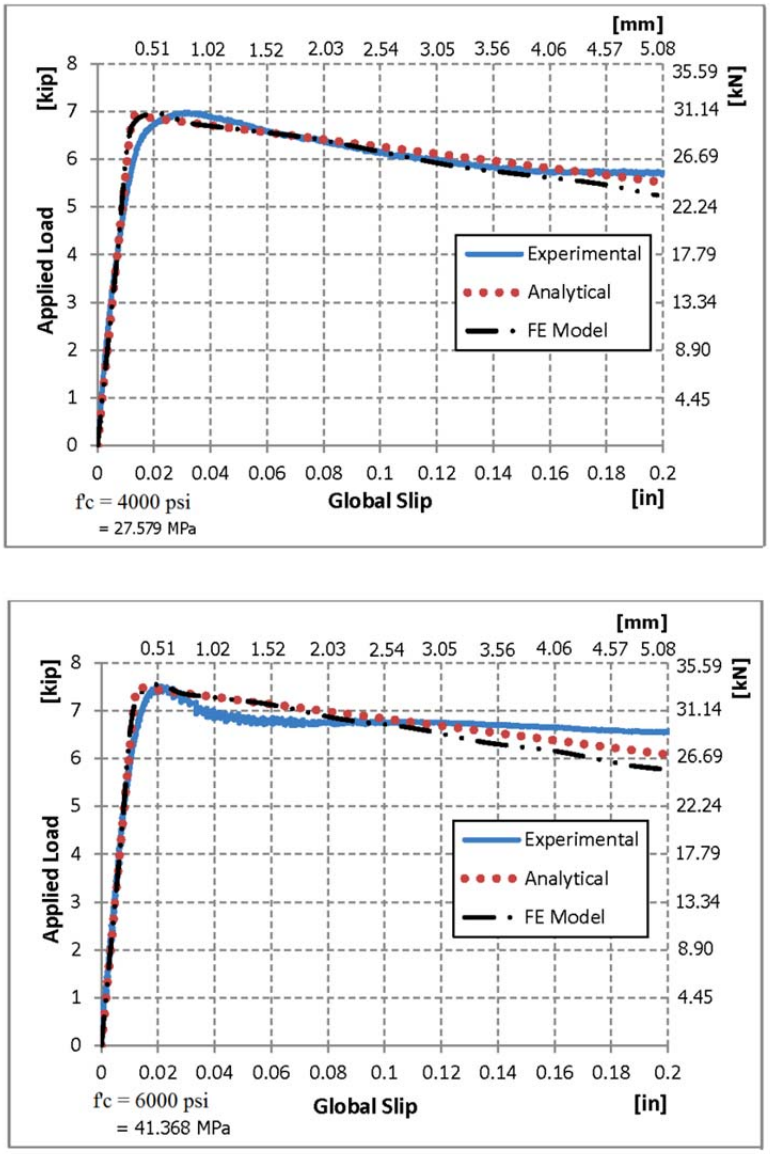

Figure 8b Results of verification

Conclusions

In this study, a local bond-slip model is developed and verified to represent the behavior of galvanized cold-formed (light gauge) steel profiles in normal weight normal strength concrete. The research begins with developing the governing mathematical equations for this specific type of bond-slip behavior by going through its mechanics. As the next step, experimental studies are performed through a new test set-up. Then an innovative procedure is introduced and followed to develop a local bond-slip model based on the obtained mathematical equations and pieces of information from the test results. Finally, the suggested local bond-slip relationship is verified to explore its validity in two ways: 1) by comparing its resulting global bond-slip graphs from analytical equations with test results. 2) by comparing its resulting global bond-slip graphs from finite element modeling with test results. An excellent agreement has been achieved in both comparisons. It is concluded that the discussed local bond-slip behavior can be expressed by a bi-linear relationship consisted of an ascending line followed by a descending line. The model's parameters can be calculated based on the value of f'c from empirical equations as suggested in this research. The proposed local bond-slip relationship can be used for the purpose of structural simulations (e.g., finite element modeling) of structures having galvanized cold-formed (light gauge) steel embedded in normal weight normal strength concrete.

Appendix A-References

Ansys Inc. (2009a). Contact Technology Guide. Canonsburg, PA: Ansys Incorporation.

Ansys Inc. (2009b). Element Reference. Canonsburg, PA: Ansys Incorporation.

Hsu, C. T. T., Munoz, P., Punurai, S., Majdi, Y., & Punurai, W. (2012). Behavior of Composite Beams with Cold-Formed Steel Joists and Concrete Slab. 21st International Specialty Conference on Cold-Formed Steel Structures, (pp. 339-353). St. Louis, MO, October 24-25.

Yuan, H., Wu, Z., & Yoshizawa, H. (2001). Theoretical Solutions on Interfacial Stress Transfer of Externally Bonded Steel/Composite Laminates. Structural Eng. / Earthquake Eng., JSCE, Vol. 18 , No. 1 , 27-39.